Mapping the dynamics of Nrf2 antioxidant and NFκB inflammatory responses by soft electrophilic chemicals in human liver cells defines the transition from adaptive to adverse responses

Braak, S.J. ter; Klip, J.E.; Wink, S.; Hiemstra, S.W.; Cooper, S.L.; Middleton, A.; ... ; Water, B. van de

Toxicology in Vitro 84 (2022) 105419

Contents lists available at ScienceDirect

Toxicology in Vitro

journal homepage: www.elsevier.com/locate/toxinvit

Mapping the dynamics of Nrf2 antioxidant and NFκB inflammatory responses by soft electrophilic chemicals in human liver cells defines the transition from adaptive to adverse responses

Bas ter Braak [a], Janna E. Klip [a], Steven Wink [a], Steven Hiemstra [a], Sarah L. Cooper [b], Alistair Middleton [b], Andrew White [b], Bob van de Water [a,*]

[a] Division of Drug Discovery and Safety, Leiden Academic Centre for Drug Research, Leiden University, Einsteinweg 55, 2333, CC, Leiden, the Netherlands
[b] SEAC, Unilever, Colworth, United Kingdom

ARTICLE INFO

Editor: Dr. P. Jennings

Keywords:
Oxidative stress
Inflammation
New approach method
Reporter assay
HepG2 BAC GFP
Dynamic regulation

ABSTRACT

A comprehensive understanding of the dynamic activation and crosstalk between different cellular stress response pathways that drive cell adversity is crucial in chemical safety assessment. Various chemicals have electrophilic properties that drive cell injury responses in particular oxidative stress signaling and inflammatory signaling. Here we used bacterial artificial chromosome-based GFP cellular stress reporters with live cell confocal imaging, to systematically monitor the differential modulation of the dynamics of stress pathway activation by six different soft electrophiles: sulforaphane, andrographolide, diethyl maleate, CDDO-Me, ethacrynic acid and tert-butyl hydroquinone. The various soft electrophiles showed differential potency and dynamics of Nrf2 activation and nuclear translocation. These differences in Nrf2 dynamics correlated with distinct activation pattern of Nrf2 downstream targets SRNX1 and HMOX1. All soft electrophiles caused a strong dose dependent suppression of a cytokine-induced NFκB response represented by suppression of NFκB nuclear oscillation and inhibition of the downstream target gene activation A20 and ICAM1, which followed the potency of Nrf2 modulation but occurred at higher concentration close to saturation of Nrf2 activation. RNAi-based depletion of RelA resulted in a prolonged presence of Nrf2 in the nucleus after soft electrophile treatment; depletion of Nrf2 caused the induction of NFκB signaling and activation of its downstream targets A20 and ICAM1. A systematic transcriptome analysis confirmed these effects by soft electrophiles on Nrf2 and NFκB signaling crosstalk in human induced-pluripotent stem cell-derived hepatocyte-like cells. Altogether our data indicate that modulation of Nrf2 by soft electrophiles may have consequences for efficient inflammatory signaling.

1. Introduction

Mechanism-based toxicity testing will become a critical component of future chemical safety testing. Test systems would integrate critical biomarkers that can quantify key events of adverse outcome pathways. With these sophisticated models it is possible to reveal the underlying toxicity pathways on top of the classical cell death end points (Niemeijer et al., 2018). These toxicity pathways would involve, among others, oxidative stress, unfolded protein response, inflammatory signaling and DNA damage responses, that may be activated by chemicals with different concentration and temporal dynamics. A chemical can induce different stress pathways each with a specific point of departure (Hiemstra et al., 2017). Given that stress pathways involved in toxicity are physiological response programs that will adapt cells, it will be critically to determine at which concentrations such adaptive programs are broken and or cross-talk between stress pathway may occur that may drive an adverse biological outcome.

We have reported previously that a large proportion of drugs with a liability for drug-induced liver injury in humans can cause the activation of the Nrf2 anti-oxidant stress response pathway (Herpers et al., 2016; Wink et al., 2017). We also observed a strong correlation between the potency to activate the Nrf2 pathway and the suppression of the expression of NFκB target genes (Fredriksson et al., 2011, 2014; Herpers et al., 2016), suggesting a direct relationship between these pathways.

* Corresponding author at: Division of Drug Discovery and Safety, Leiden Academic Centre for Drug, Research, Leiden University, Einsteinweg 55, 2333, CC, Leiden, the Netherlands.
E-mail address: b.water@lacdr.leidenuniv.nl (B. van de Water).

https://doi.org/10.1016/j.tiv.2022.105419
Received 3 January 2022; Received in revised form 19 May 2022; Accepted 14 June 2022
Available online 17 June 2022

Interaction of the Nrf2 and NFκB signaling is supported by the fact that the promotor region of the Nrf2 gene (NFE2L2) has several functional NFκB binding sites (Rushworth et al., 2014)(Rushworth et al., 2011). In addition, Nrf2 knockout mice are more sensitive towards cytokine-induced inflammation (Thimmulappa et al., 2006) and Nrf2 counters transcriptional regulation of pro-inflammatory genes (Kobayashi et al., 2016). Currently, a systematic evaluation of the consequences of chemical-induced Nrf2 activation on inflammatory signaling by NFκB has so far been lacking. Since modulation of the Nrf2 pathway is a critical pharmacological target, suppression of inflammatory at equal potent levels could lead to unanticipated activities. We used a panel electrophiles to investigate such a relationship in detail.

Electrophiles are chemical entities that are either positively or neutrally charged which can covalently bind with negatively charged nucleophiles. These reversible electrophile-nucleophile interactions, also known as redox signaling, are very important physiologically (Burgess et al., 2016). However, when the ratio of electrophiles (e.g. reactive oxygen species) and nucleophiles (e.g. antioxidants) is increased this might lead to cytotoxicity. Based on their polarizability electrophiles can be divided into soft or hard electrophiles. Hard electrophiles will react with hard nucleophiles (e.g. aromatic nitrogen sites on DNA bases) controlled by charge and therefore might cause DNA damage. Soft electrophiles are more prone to react with soft nucleophiles (e.g. a sulfhydryl thiol side-chain of cysteine residues) predominantly controlled by orbital. Soft electrophiles will induce an Nrf2 response by adduct formation with sentinel cysteine residues on Kelch-like ECH associated protein 1 (KEAP1) which leads to dissociation and subsequent nuclear translocation of Nrf2, eventually leading to the activation of the oxidative stress response (Lopachin and Gavin, 2017) (Yamamoto et al., 2018). We have established a panel of GFP reporter HepG2 cell lines to monitor the cellular stress response pathways. These reporters were established using bacterial artificial chromosome-based genome engineering and contain the gene of interest (e.g. a biomarker for cellular stress) with its regulatory subunits (>10 kb up and downstream of gene target) fused to GFP to ensure endogenous expression (Poser et al., 2008) (Wink et al., 2014). Using this reporter panel in combination with live cell microscopy and automated image segmentation/quantification we can follow the dynamic activation of specific biomarkers of various cellular stress response pathways. In this study we used reporters for the Nrf2 antioxidant stress response pathway (Nrf2-BAC-GFP, SRXN1-BAC-GFP and HMOX1-BAC-GFP), the NFκB inflammatory response pathway (RelA-BAC-GFP, IκBα-BAC-GFP, A20-BAC-

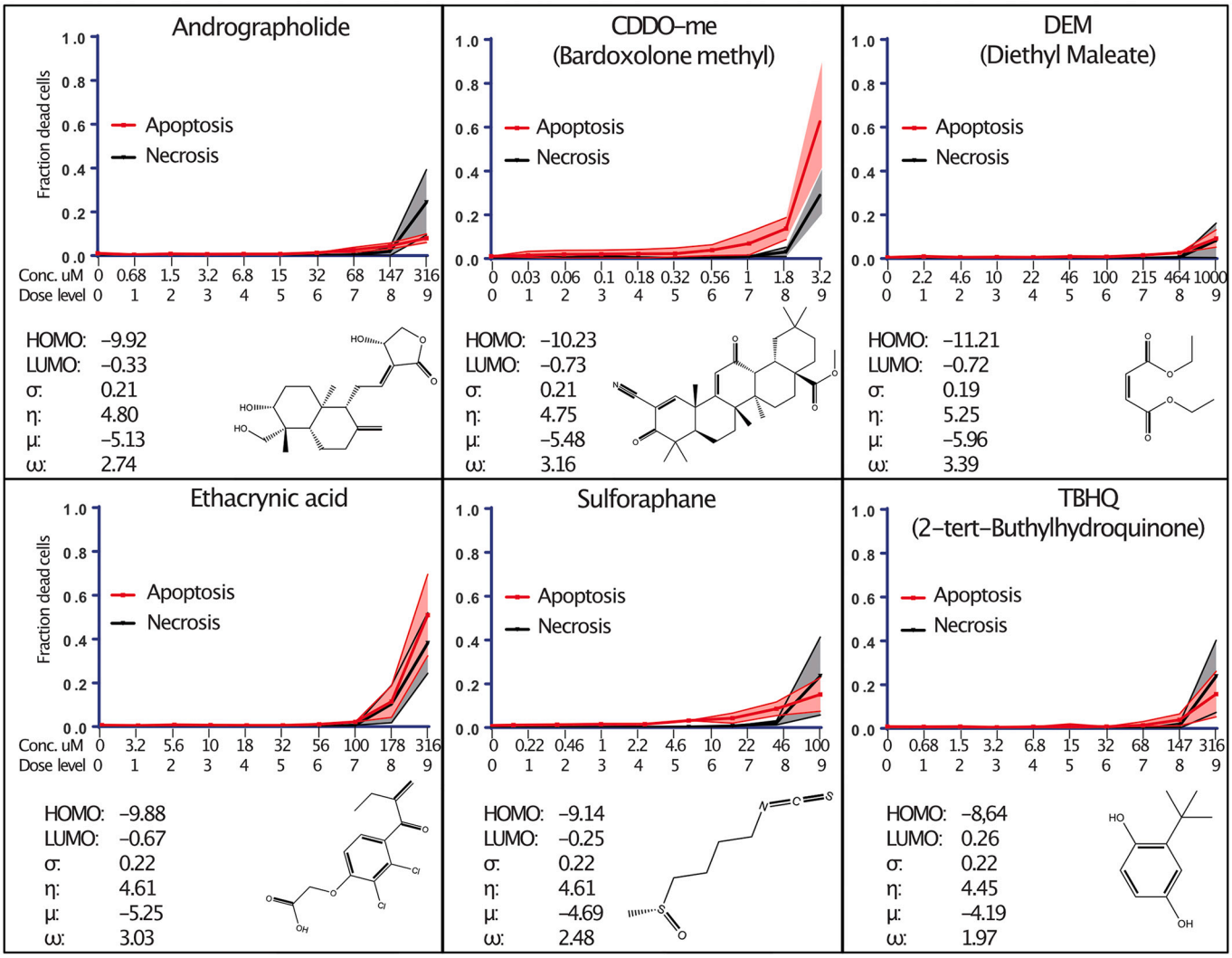

Fig. 1. Physicochemical characteristics and cytotoxicity potency of six soft electrophiles. For each compound 9 concentrations have been tested. Cell death, apoptosis (AnV in red) and necrosis (PI in black), were evaluated for each compound in the HepG2 wild type cell line. The lines represent the mean of biological triplicates with the standard deviation presented as the light colored panel. Below the 2D representation of the chemical structures and several HSAB parameters of each compound are listed: Chemical hardness (η), chemical softness (σ), chemical potential (μ) and Electrophilic index (ω). (For interpretation of the references to color in this figure legend, the reader is referred to the web version of this article.)

GFP and ICAM1-BAC-GFP). Since some chemicals that activate the Nrf2 pathway also affect the protein folding in the endoplasmic reticulin (Wink et al., 2017), we also involved reporters that can report on the activation of the unfolded protein response pathway (BIP-BAC-GFP, CHOP-BAC-GFP).

In this study we systematically investigated the cross talk between the Nrf2 and NFκB pathways during chemical exposure. We used six test soft electrophilic compounds with different structures and physical-chemical properties: andrographolide, bardoxolone methyl (CDDO-me), diethyl maleate (DEM), ethacrynic acid, sulforaphane and tert-butylhydroquinone (TBHQ) (Fig. 1). These test compounds activate the Nrf2 pathway through modulation of cysteine residues in Keap1, albeit with different potencies (Li et al., 2018)(Wu et al., 2010) (Turley et al., 2016). In addition, these compounds have been linked to suppression of inflammatory signaling (Guerrero-Beltrán et al., 2012; Han et al., 2005; Jones et al., 1999; Srivastava and Akhila, 2010). We established detailed concentration and time course landscapes for Nrf2 and NFκB pathway HepG2 reporter cell lines after exposure with six soft electrophiles. RNA interference was used to mechanistically understand the interactions between these pathways. Finally, targeted RNA sequencing was used to generalize our findings in HepG2 cells to other liver cell test systems.

2. Materials and methods

2.1. Reagents and chemicals

Human TNFα purchased from R&D systems (United Kingdom) and Human Interleukin-1 ProSpec (Germany) were dissolved in 0.1% BSA/PBS. All other compounds were purchased at Sigma-Aldrich (The Netherlands) and dissolved in DMSO. Aliquots were stored at −20 °C. At the highest exposure the DMSO concentration was equal or <0.2% (*v*/v).

2.2. Chemical characteristics

The significant degree of selectivity that occurs in electrophile-nucleophile interactions is predicted by Pearson's Hard and Soft, Acids and Bases (HSAB) theory. The highest energy orbital that contains electrons, HOMO (Highest Occupied Molecular Orbital) and the lowest energy orbital that is vacant, LUMO (Lowest Unoccupied Molecular Orbital). These energies are determined using the fast semi-empirical Austin Model 1 (AM1) using MOPAC implemented into TIMES software. The calculations are done for all possible conformers, so for HSAB parameters' calculation the max, min or average HOMO and LUMO energies can be applied. Hardness $\eta = [E_{LUMO} - E_{HOMO}]/2$, Softness $\sigma = 1/\eta$, Chemical potential $\mu = [E_{LUMO} + E_{HOMO}]/2$, Electrophilic index $\omega = \mu^2/2\eta$. Chemical structures have been drawn with http://www.chemspider.com, converted with Chem3D pro version 16.0.0.82 and exported to .svg.

2.3. Cells and culture conditions

The original human hepatoma HepG2 cell line, clone HB8065, was acquired from ATCC (Germany). Previously we have generated reporter cell lines to visualize and quantify the induction of several adaptive stress pathways (Wink et al., 2014). These BAC-GFP reporters have integrated the full regulatory sequences (>10 kb) up and downstream of the target gene to ensure endogenous expression. This biomarker gene was C-terminally fused to an eGFP sequence. These cells were maintained and exposed to compounds in full medium (DMEM high glucose medium supplemented with 10% (*v*/v) FBS, 25 U/mL penicillin and 25 μg/mL streptomycin). Cells were used between passage 14 and 20.

hiPSC derived hepatocytes (Cellartis, enhanced hiPSC-HEP from ChiPSC18, cat#Y10051 Lot# AH200015) were cultured according to manufactures instructions. In short; 128,000 cells/well were seeded in a 96-well plate, cultured for 7 days on maintenance medium. For the exposures, compounds were dissolved in maintenance medium.

2.4. Cell treatment

For live-cell imaging, the HepG2 BAC-GFP reporter cells were seeded in Greiner Bio-One (The Netherlands) black μ-clear 384-well plates with 8.000 cells per well. 1 day after attachment, the cells were incubated for two hours with 100 ng/mL $Hoechst_{33342}$. Subsequently the Hoechst was removed and compounds were added in full medium in a wide concentration range (indicated in Fig. 1). To evaluate the onset of cell death, the medium also contained 0.05% AnnexinV−Alexa633 (marker for apoptosis) and 100 nM propidium iodide (marker for necrosis).

For the sequencing experiment hiPSC-Heps and HepG2 wildtype (wt) were exposed to four compounds at six concentrations (andrographolide; 146, 68, 31.6, 14.67, 6.8, 3.16 μM, CDDO-me; 1.78, 1.0, 0.56, 0.32, 0.18, 0.1 μM, sulforaphane; 46.4, 21.54, 10.0, 4.64, 2.15, 1.0 μM and TBHQ; 146, 68, 31.6, 14.67, 6.8, 3.16 μM). 16 h after exposure cells were harvested by removing medium and adding 1× Biospyder lysis buffer. TNFα (10 ng/mL) or IL1β (5 ng/mL) was added 8 h prior to harvesting. For the hiPSC-Heps the compounds were dissolved in maintenance medium, for HepG2 exposures full DMEM medium was used.

2.5. Live cell confocal microscopy and quantification of HepG2 BAC-GFP activation

To assess the effect of compound exposure on the dynamic stress response activation we used live cell confocal imaging. Directly after compound exposure the cells were imaged using Nikon TiE2000 including an automated xy-stage, an integrated Perfect Focus System (Nikon, Amsterdam, The Netherlands), and 408, 488, 561, and 647 nm lasers. After 24 h image acquisition the data file (.nd2) was retrieved and exported as .tiff files. We used ImageJ (version 1.51o) to create a binary image of the Hoechst channel using an in house made plugin based on a watershed based segmentation algorithm (Di et al., 2012). Subsequently, CellProfiler (version 2.2.0) was used to propagate the cytoplasmic area based on the Hoechst binary and overlay the binary Hoechst/GFP channel and or the binary cytoplasm/GFP channel to quantify per segmented pixel the GFP intensity. The sum of these intensities is referred to as the integrated GFP intensity in the nucleus (Nrf2) or in the cytoplasm (SRXN1, HMOX1, ICAM, A20) (ter Braak et al., 2021b). For the nuclear translocation of RelA (subunit of the p65 complex) and IκBα (inhibitor of this complex), nuclei are tracked in CellProfiler and for each time point the normalized nuclear/cytoplasmic GFP intensity ratio was determined on a single cell basis.

2.6. Targeted sequencing and data processing

Prior to lysis, medium was removed, cells were washed with PBS and 1× BioSpyder (BS) lysis buffer was added. Plates were stored at −80 °C and sent to BioSpyder for further processing.

Gene expression profiles were determined using a targeted RNA sequencing technology, TempO-Seq (Biospyder technologies, Inc., Carlsbad, CA, USA) (Yeakley et al., 2017). In short, expression profiles of in total 2981 genes were analyzed. These selected genes provide maximal mode-of-action information on chemical perturbations that reflect general cellular stress. Reads were aligned using TempO-seqR package, raw counts were normalized and log transformed using the DESeq2 package. The primary human hepatocyte (PHH) data in the Open TG-GATEs dataset was used to determine the top 25 genes associated with a NFκB response in human liver cells, the same was done for the top 25 genes associated with a Nrf2 response. Of these 50 genes for each pathway the top 15 were selected based on fold change expression and a minimum normalized base expression count of 10 within the hiPSC-Heps and visualized as a heatmap (Fig. 6). Principle Component Analysis (PCA) plots were generated using the prcomp function from the

Stats R package. Rstudio version 1.0.153 (Boston, USA) in combination with R version 3.4.1 was used in combination with the following visualization packages (pheatmap (Kolde, 2012), ggplot2 (Wickham, 2009)).

2.7. Statistics

For the time response graphs an independent two-sided Welch Student's *t*-Test was performed with the area under the curves (AUC), each comparison was compared to the siCtrl condition. The AUCs were calculated with the trapezoid method using the R pracma package 2.2.2. In the figures the significance is indicated with asterisks (ns = $p > 0.05$, * = $p \leq 0.05$, ** = $p \leq 0.01$, *** = $p \leq 0.001$).

3. Results

3.1. Cytotoxicity and electrophilic properties of the compound set

We evaluated the cellular stress response activation of six different soft electrophiles: andrographilide, bardoxolone-methyl (CDDO-me), diethylmaleate (DEM), ethacrynic acid, sulfphoraphane and tert-butylhydroquinone (TBHQ) (Fig. 1). These compounds were selected based on the divergence of their chemical structures and their range of electrophilic reactivity. The electrophilic index (ω) is a parameter that combines softness (σ) and chemical potential (μ) and reflects the propensity of the electrophile to form adducts with a given biological nucleophile (e.g. KEAP1). These measurements predict that DEM has the highest electrophilic reactivity and TBHQ has a lower potential to form adducts and thus activate the Nrf2 pathway. Next, we established the testing concentration range of the different compounds. We aimed for a concentration range that induced activation of adaptive stress response rather than cytotoxicity. With cell death markers we tested apoptosis (AnV) or necrosis (PI) in parental HepG2 cells. Only at the highest concentration(s) we observed some cell death for several soft electrophiles, with clear differences in potency: CDDO-Me > > ethacrynic acid > TBHQ = sulforaphane = andrographolide > DEM.

3.2. High content live cell dynamics of Nrf2 mediated oxidative stress response reporters

Next, we evaluated the dynamics of cellular stress response activation using live cell imaging (Fig. 2A/B) with evaluation of cell count (Hoechst), cell viability (PI) and cellular stress response reporter activity (GFP). We first determined the activation of the Nrf2 pathway by measuring Nrf2 stabilization and nuclear translocation as a consequence of KEAP1 modulation by the soft electrophiles as well as Nrf2-mediated induction of Srxn1 and HMOX1 (Fig. 2C). Soft electrophiles increased the nuclear Nrf2-GFP levels for all soft electrophiles as exemplified by DEM which peaked at 5 h and slowly declined in the following period. This Nrf2 dynamic response was linked to a gradual increase of cytoplasmic SRNX1-GFP and HMOX1-GFP, which was initiated after peak Nrf2 levels were reached. Quantification of the Nrf2 activation landscape showed clear concentration response effects for all test compounds in all reporters indicating that all tested electrophiles induce an oxidative stress response (Fig. 2D; Suppl. Fig. 1). Of relevance, the dynamics of Nrf2 nuclear translocation was very different among the compounds. Andrographolide exposure caused a very strong nuclear translocation of Nrf2 with a peak at ~12 h and a subsequent strong induction of both SRXN1 and HMOX1. In contrast, CDDO-me caused a mild, yet sustained, activation of Nrf2 and upregulation of SRXN1, but a very strong induction of HMOX1 at high concentration. Sulforaphane showed strong, yet transient, activation of Nrf2 at high concentration and subsequently the SRXN1 reporter; only a very mild activation of HMOX1 was observed. DEM, ethacrynic acid and TBHQ show a similar and mild oxidative stress activation pattern. Overall, SRXN1 induction was observed at concentration that did not yet activate a HMOX1 response.

3.3. High content live cell dynamics of NFκB mediated inflammation response reporters

We further investigated the implication of soft electrophilic compound treatment on the activity of NFκB signaling response (Fig. 3A-B). Here we used inflammatory signaling reporters that can monitor the temporal dynamics of cytokine-mediated activation of the NFκB pathway: RelA-GFP, IκB-GFP, A20-GFP and ICAM-GFP reporter cell lines (Fig. 3C-D). The reporter cells were first treated with the different electrophiles for 8 h, a time point where maximal activation of Nrf2 activation was reached; thereafter either TNFα or IL-1β was added. Under control conditions virtually all RelA-GFP was present in the cytoplasm and after TNFα exposure the majority of RelA-GFP did translocate to the nucleus with a maximum at around 30 min, and thereafter oscillating between the cytosol and the nucleus (Fig. 3D). This was associated with an inverse oscillation cycle of the IκBα-GFP levels (Fig. 3D inserts). In Fig. 3C the representitative images of just four timepoints are shown, which is not enough to appreciate this oscillatory effect. Therefore we have uploaded movies of the dynamic responses of the different reporters in which the dynamic acitvation upon exposure to Diethyl Maleate (oxidative stress reporters) or TNFα (inflammation reporters) can be appreciated (*https://www.youtube.com/playlist?list=PLp3gUC3ds9u3s0xYmgOP-jqPB8eXv1Pv5*). Furthermore we previously described this oscillatory effect of the RelA-GFP in detail (Fredriksson et al., 2011). Pretreatment with the six electrophiles caused a concentration dependent disruption of this oscillatory behavior, which was associated with a decrease in the first NFκB nuclear translocation (andrographolide and CDDO-Me) and/or a delay of the overall oscillatory response at later time points (andrographolide, CDDO-Me, sulphoraphane) or even a sustained accumulation of NFκB in the nuclear compartment without full relocation to the cytosol (DEM, ethacrynic acid). Interestingly, the amplitude of the first peak after ethacrynic acid exposure was increased. Given the perturbation of the NFκB oscillatory response, we also assessed whether the diverse soft electrophiles also impacted on the TNFα-induced expression of downstream κtarget genes, A20/TNFAIP3, an early response target gene, and ICAM1, a late response target gene (Lerebours et al., 2008). We made advantage of the A20-GFP and ICAM1-GFP reporters. TNFα caused a drastic sharp increase in A20-GFP which leveled off after around 4 h to a new steady state A20-GFP expression. ICAM1-GFP induction by TNFα had a delay of around 4 h and followed a sustained expression for the 24 h time period. All compounds demonstrated an almost complete inhibition of both ICAM1-GFP and A20-GFP induction by TNFα. A full concentration dependent inhibition of TNFα-mediated ICAM1-GFP induction was in particular observed for andrographolide, CDDO-Me, DEM and ethacryinic acid. We next determined whether this effect did also involve other cytokine-mediated activation of NFκB. IL-1β also caused the oscillatory response of RelA-GFP and IκB-GFP, which was inhibited by the soft electrophiles in a similar dose response as observed for TNFα (Suppl. Fig. 3). Moreover, also a concentration dependent inhibition of IL-1β-mediated A20-GFP and ICAM1-GFP was observed (Suppl. Fig. 4). Together these data indicate a consistent impact of soft electrophiles on cytokine-mediated NFκB signaling with strong association with modulation of the oscillatory degradation of IκB and nuclear transloction of NFκB.

3.4. Comparison of modulation of the different cellular stress response pathways by soft electrophiles

Soft electrophiles can also impact on the cellular redox status that might affect for example the folding of proteins. In particular the endoplasmic reticulum is sensitive to altered redox potential (Higa and Chevet, 2012), causing the accumulation of unfolded newly translated proteins causing the activation of the unfolded protein response (UPR). Therefore, next we followed the activation of the UPR using our previously established UPR reporters, BiP-GFP and CHOP-GFP in a similar

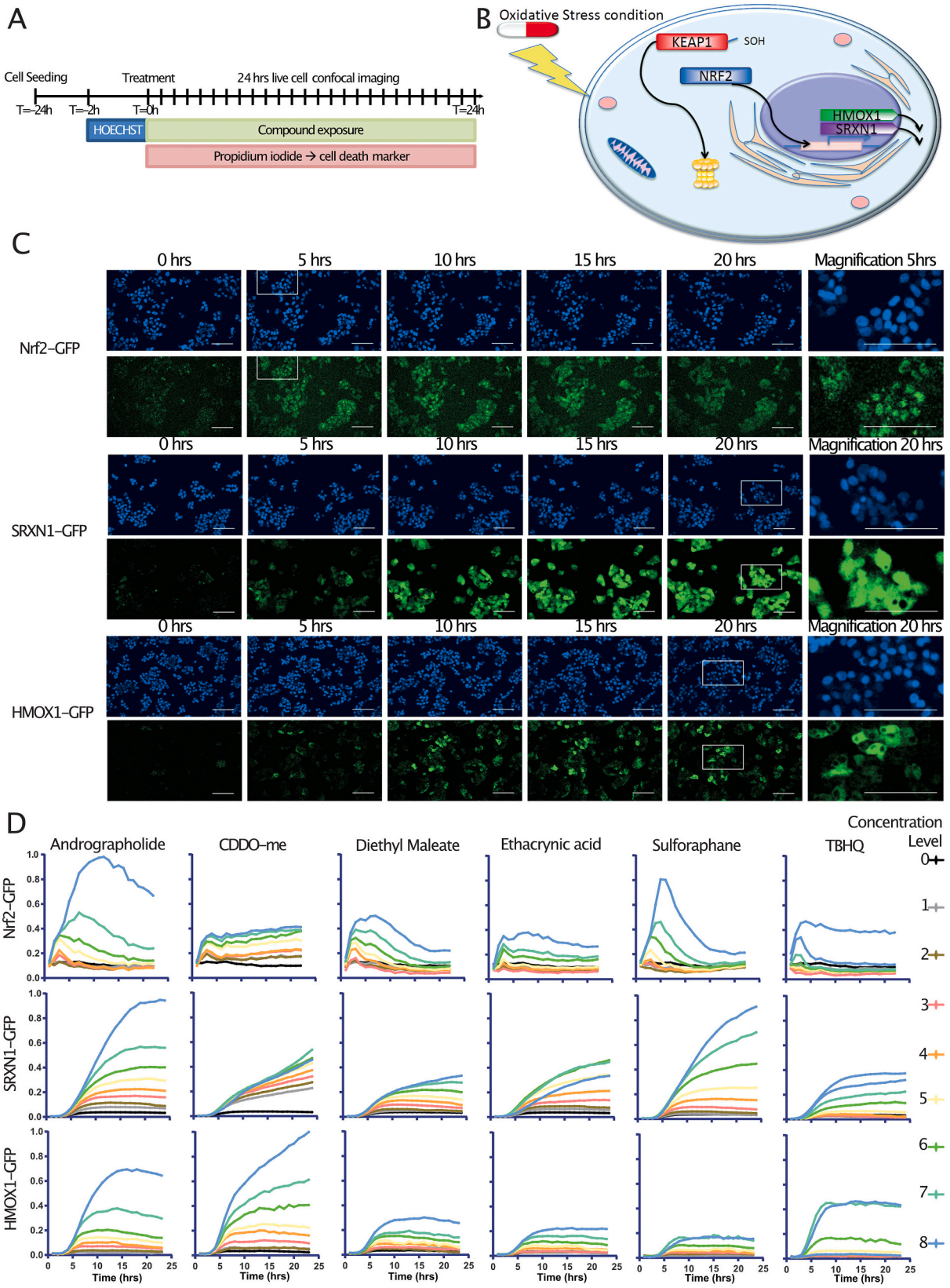

Fig. 2. Induction of Nrf2 pathway reporters by different soft electrophiles. A) Schematic overview with the time line and experimental procedures. B) Schematic overview of the Nrf2 pathway with the different GFP-tagged biomarkers and their subcellular localization in an oxidative stress condition. C) Representative confocal images of Nrf2-GFP, SRXN1-GFP and HMOX1-GFP induction over time upon stimulation with 464 μM diethyl maleate. The last image of each row represents a magnified region that corresponds with the white square in one of the pictures in that series. White scale bars in the lower right corners of the confocal images represent 200 μm. D) Quantification (integrated GFP intensity) of the confocal images in time response curves. Each row represents data of one of the oxidative stress reporters (Nrf2-GFP, SRXN1-GFP and HMOX-GFP) and each column represents data of one of the six soft electrophiles.

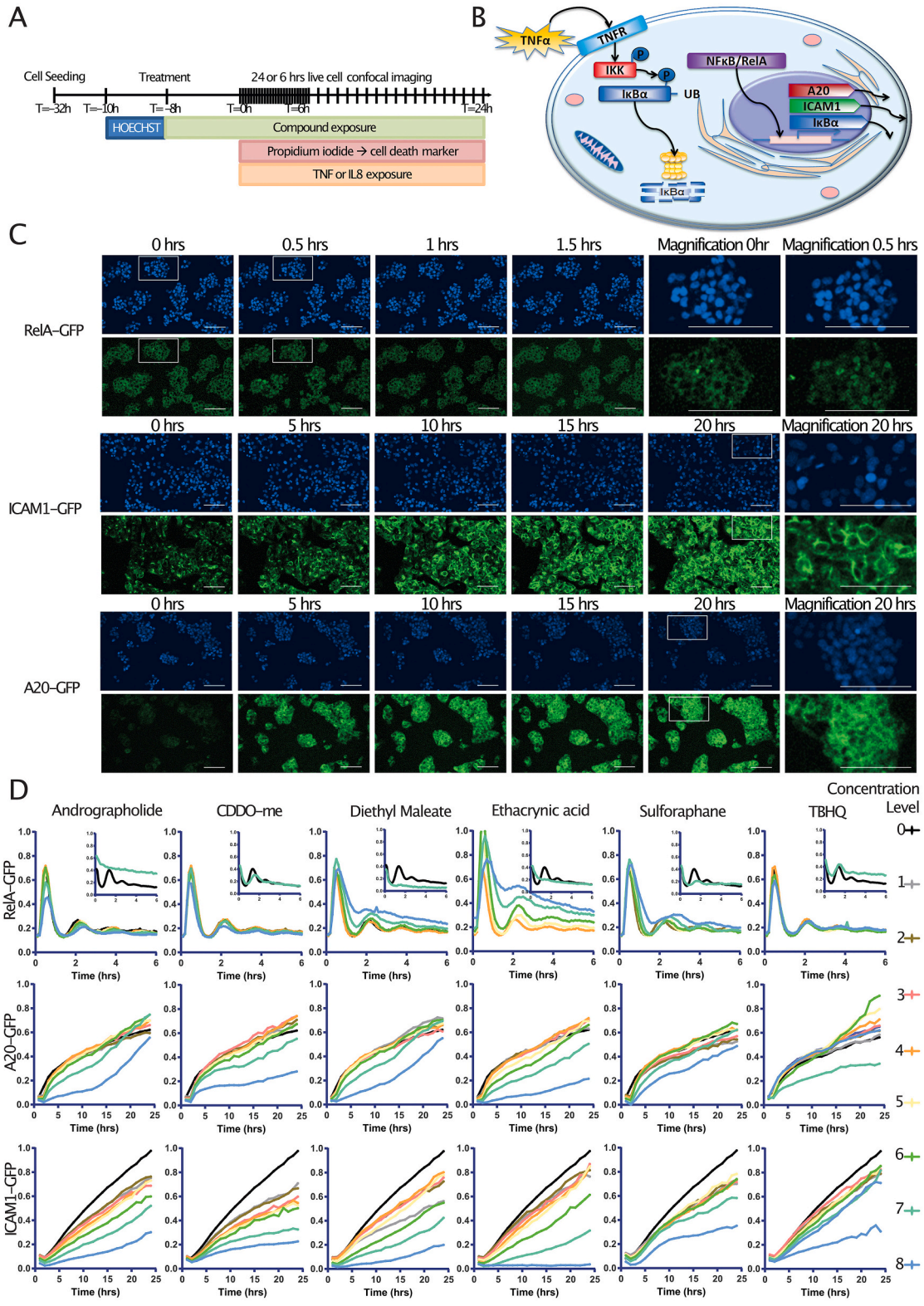

Fig. 3. Inhibition of the TNFα-mediated inflammatory response by soft electrophiles. A) Schematic overview with the time line and experimental procedures. B) Schematic overview of the NFκB pathway with the different GFP-tagged biomarkers and their subcellular localization in Inflammatory condition. C) Representative time course confocal images of RelA-GFP, ICAM1-GFP and A20-GFP induction upon exposure to 10 ng/mL TNFα. The last image of each row represents a magnified region that corresponds with the white square in one of the pictures in that series. White scale bars in the lower right corners of the confocal images represent 200 μm. D) Quantification of the dynamic reporter activation in time response curves. Each row represents data of one of the inflammation reporters (RelA-GFP, A20-GFP and ICAM-GFP) and each column represents data of one of the six soft electrophiles. Note that the insert in top panel of the RelA curves reflect the behavior of IκBα-GFP reporter activity at the highest concentration.

manner as for the Nrf2 and NFκB pathway reporters. We observed BiP-GFP activation only for CDDO-Me, but not for the other soft electophiles (Fig. 4). In contrast, all compounds induced the activation of CHOP-GFP, but this was observed only at the highest concentrations where the Nrf2-mediated activation of Srxn1-GFP was already suppressed. Onset of the CHOP-GFP induction was observed at similar levels as the suppression of the cytokine-induced A20-GFP expression, yet at slightly higher concentrations than HMOX1-GFP induction. In contrast, Nrf2 was already activated at low concentration and associated with a concentration-dependent activation of SRXN1-GFP in a similar concentration range. Activation of SRXN1-GFP showed a very small concentration window where the TNFα- and IL1β-induced ICAM1-GFP expression was unaffected (Fig. 4). Interestingly, in the absence of cytokines, A20 was increased at the highest soft electrophile concentrations, indicating that at these high concentrations A20 expression can be induced. We also monitored the association with onset of cytotoxicity and only observed some toxicity at the highest concentration. Interestingly, addition of TNFα and IL1β had a protective effect against cell death. The integrated data demonstrated that the cellular stress signaling activation patterns of andrographolide and sulforaphane were most similar to each other. Also the activation profiles of DEM and ethacrynic acid shared stronger resemblance. Overall, TBHQ was the least active compound and only impacted on Nrf2 activation and inhibition of NFκB signaling at the highest concentrations.

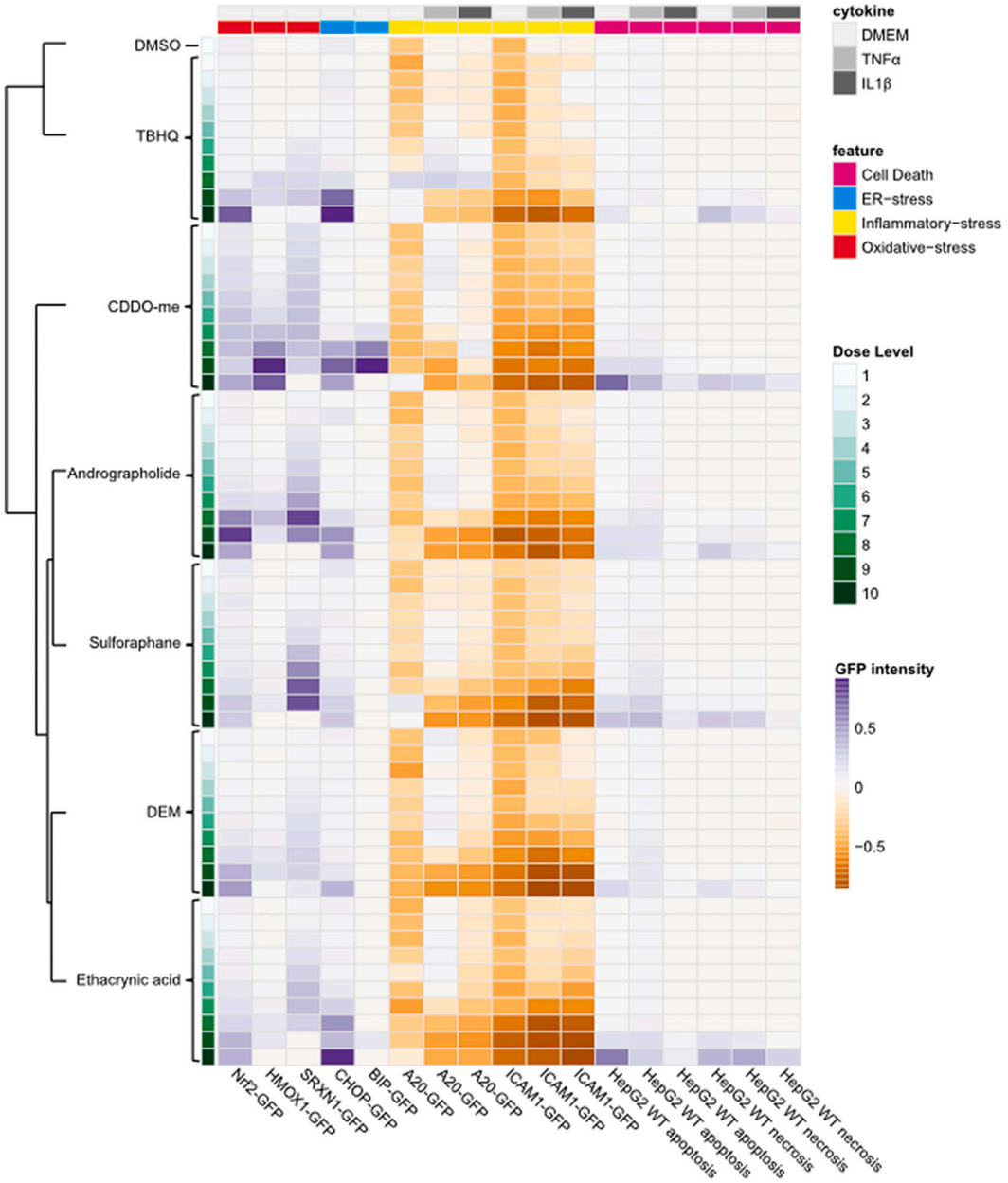

Fig. 4. Heatmap with hierarchical clustering with data from the HepG2 BAC GFP reporters exposed to soft electrophiles. Each cell contains a color that represents the GFP intensity of the areas under curves (AUCs) of the dynamic reporter-GFP plots. Each column represents data of inflammation reporters (A20/ICAM1), oxidative stress reporters (Nrf2/HMOX1/SRXN1, ER stress reporters (CHOP/BIP) or cell death markers (PI/AnV). For the inflammation reporters the DMEM, TNFα and IL1 conditions are shown. The data is min-max scaled, at which the highest induction and reduction (often in CDDO-me) was set to 1 and − 1, respectivly. The DMSO treatment was set to 0, but for the inflammation reporters the DMSO+TNFα condition was used as the minimal reference point so that effects of cytokine induced NFκB signaling could be determined.

3.5. Functional interaction between Nrf2 and NFκB pathway during soft electrophile treatment

Given the effect soft electrophiles have on both Nrf2 and NFkB signaling in the lower concentration range, we further investigated the possible crosstalk between the NFκB and Nrf2 pathway. Since DEM showed the clearest concentration response inhibition of TNFα-induced ICAM1-GFP expression, for these studies we used co-treatment of DEM and TNFα. First, we depleted Nrf2 and RelA using siRNA transfection in the different reporters and exposed the cells to different concentration of DEM. Nrf2 depletion prevented Nrf2-GFP accumulation in the nucleus in association with an almost complete inhibition the DEM-mediated induction of SRXN1-GFP (Fig. 5B). Knockdown of Nrf2 also suppressed the TNFα-mediated induction of ICAM-GFP, but not the early onset of A20-GFP expression. Depletion of RelA did not completely abrogate the induction of A20-GFP and ICAM1-GFP by TNFα, as expected. Of interest, RelA knockdown also suppressed the SRXN1-GFP induction caused by DEM, while Nrf2-GFP was slightly more stabilized over time (Fig. 5B). We also investigated the effect enhanced activation of Nrf2 and NFκB signaling pathways, and used depletion of KEAP1 and A20, negatively regulators of both pathways respectively. KEAP1 depletion caused a reduction of ICAM1-GFP induction by TNFα (Fig 5C_{ii}), which was associated with an enhanced induction of A20-GFP, suggesting a role for Nrf2 in modulating A20 levels, and thereby controlling cytokine-mediated activation of NFκB signaling. Depletion of A20, thereby providing a more sustained cytokine-mediated activation of NFκB, did cause a more sustained stabilization of Nrf2-GFP levels, but suppressed SRXN1-GFP induction in a similar fashion and RelA depletion (Fig. 5D). To further understand the interaction of Nrf2 signaling on NFκB activation, we studied the TNFα-induced RelA/NFκB cytoplasmatic to nuclear oscillatory behavior under knockdown conditions (Fig 5C_{iii}). Depletion of A20 caused an increase of nuclear RelA-GFP as indicated by the increased area under the curve (AUC), confirming the negative feedback loop of A20 to NFκB (Afonina et al., 2017). Depletion of Nrf2 also caused an increased nuclear levels of RelA-GFP. Loss of KEAP1 slightly enhanced the nuclear translocation dynamics of NFκB. Based on the above results we postulate a direct subtle interaction between Nrf2 and NFκB (Fig. 5E).

3.6. Transcriptional profiling of soft electrophile responses in HepG2 and hiPSC-Heps

As a final step we wanted to evaluate if the interaction between soft electrophile responses on the Nrf2 and NFkB pathways was also evident in other liver test systems. Although a first choice would be primary human hepatocytes, we have observed that this test system has limitations in the sensitivity to detect inflammatory signaling. In contrast, human iPSC-derived hepatocyte like cells (hiPSC-Heps) are highly responsive to TNFα (ter Braak et al., 2021a). Therefore, we compared the transcriptional response of HepG2 cells and hiPSC-Heps to soft electrophiles and TNFα using targeted sequencing as indicated (Fig. 6A). We confirmed that soft electrophiles caused the induction of various hallmark Nrf2 target genes (SRXN1, HMOX1, GCLM and GCLC) in both HepG2 (Fig 6Bi) and hiPSC-Heps (Fig 6Bii). The HepG2 model was more sensitive for induction of the Nrf2 target genes than the hiPSC-Heps. When comparing fold changes of the TNFα response we also observed that in both test systems andrographolide did inhibit the TNFα-induced induction of hallmark NFκB downstream target genes (ICAM1, TNFAIP3, BIRC3 and CXCL1) (Fig. 6B). Important to note is that exposure with TNFα did not affect any of the Nrf2 target genes itself in HepG2 or hiPSC-heps. In contrast, as anticipated, the NFκB target genes were all significantly induced by TNFα treatment. Remarkably, fold change induction of NFκB target genes did range between 6 and 20 fold in HepG2, and only 1.2–2.7 fold in hiPSC-Heps (Fig. 6C). Yet, despite the difference between the two test systems, the suppression of the TNFα response by andrographolide was similar (Fig. 6B). We further evaluated the concentration response effect of four different soft electrophiles (andrographolide, CDDO-me, sulforaphane and tBHQ) on the expression of a broader panel of Nrf2 and NFκB responsive genes in hiPSC-Heps. Hierarchical clustering demonstrated a perfect separation in the response between expression levels of the NFκB (in red) and Nrf2 (in blue) target genes. All four soft electrophiles caused a concentration dependent upregulated of the Nrf2 target genes and a downregulation of NFκB target genes (Fig. 6D). The suppression of NFκB target gene expression typically occurred at higher concentration than the Nrf2 target gene induction, but responses differed per target gene. Overall this transcriptomics evaluation indicate that the soft electrophiles induce an Nrf2 mediated oxidative stress response and reduce the NFκB pathway in hiPSC-Heps.

4. Discussion

In the study we determined the effects of six different soft electrophilic chemicals, CDDO-me, andrographolide, sulforaphane, ethacrynic acid, DEM and TBHQ, that has a primary mode-of-action target the Nrf2 pathway. For this purpose we made advantage of a HepG2 fluorescent protein reporter panel and live cell confocal imaging to monitor the activation of cellular stress response pathways, including the Nrf2 pathway, the cytokine-mediated activation of the NFκB pathway and the unfolded protein response. Our key findings are that all chemicals rapidly induce the nuclear accumulation of Nrf2 at low concentrations followed the initiation of activation of the downstream target SRXN1. At higher concentrations these soft electrophiles inhibit the nuclear translocation of the TNFα- and IL-1β-induced NFκB, which is associated with the inhibition of the induction of A20 and ICAM1. At higher sub-cytotoxic concentrations the electrophiles induce the activation of other stress pathways, including the unfolded protein response, CHOP and BiP as well as HMOX1. Finally, these observations were confirmed by transcriptome analysis in both HepG2 and human iPSC-derived hepatocyte like cells.

CDDO-me, sulforaphane and andrographolide have potent beneficial pharmacological activity on Nrf2 pathway activation allowing cytoprotection of cells against oxidative stress (Guerrero-Beltrán et al., 2012). For this reason, CDDO-me has been studied in clinical trials to induce improved renal function based in chronic kidney disease patients (Zeeuw De et al., 2013). Soft electrophilic properties are not without any hazard, as is evidenced by the adverse outcome pathway of skin sensitization (Patlewicz et al., 2014), for which the ARE-Nrf2 luciferase reporter has been evaluated for sensitization screening (Maeda et al., 2020). Our data supports different concentration ranges of biological activity for relevant cellular stress response pathways. We anticipate that an adaptive Nrf2 pathway is activated at low concentrations of the soft electrophiles, where modifications of KEAP1 Cys residues are highly sensitive sensors to initiate an antioxidant response and protect cells against stress. At higher concentrations, while the Nrf2 pathway activation is stronger, we also observed a transition towards an unanticipated modulation of other stress response pathway, with suppression of cytokine-mediated NFκB activation being more susceptible than the unfolded protein response. Thus, our data indicate that KEAP1 targeting soft electrophiles have a safe range that selectively activates the Nrf2 pathway. However, at higher concentration these molecules may also affect other pathway that may increase a risk for adverse effects. We anticipate that our combined panel of BAC-GFP HepG2 Nrf2 and NFκB pathway reporter panel is an excellent test system to determine the point-of-departure for Nrf2 and NFκB pathway modulating properties of soft electrophiles and other chemicals.

We used in silico approaches to calculate the electrophilic index of our six model compounds. This index is an indication for the potential to form adducts with KEAP1 and thus induce an Nrf2 response. This method ranked our compounds from high to low electrophilic index: DEM, CDDO, ethacrynic acid, andrographolide, sulforaphane and TBHQ. In contrast, based on our in vitro reporter assays for Nrf2

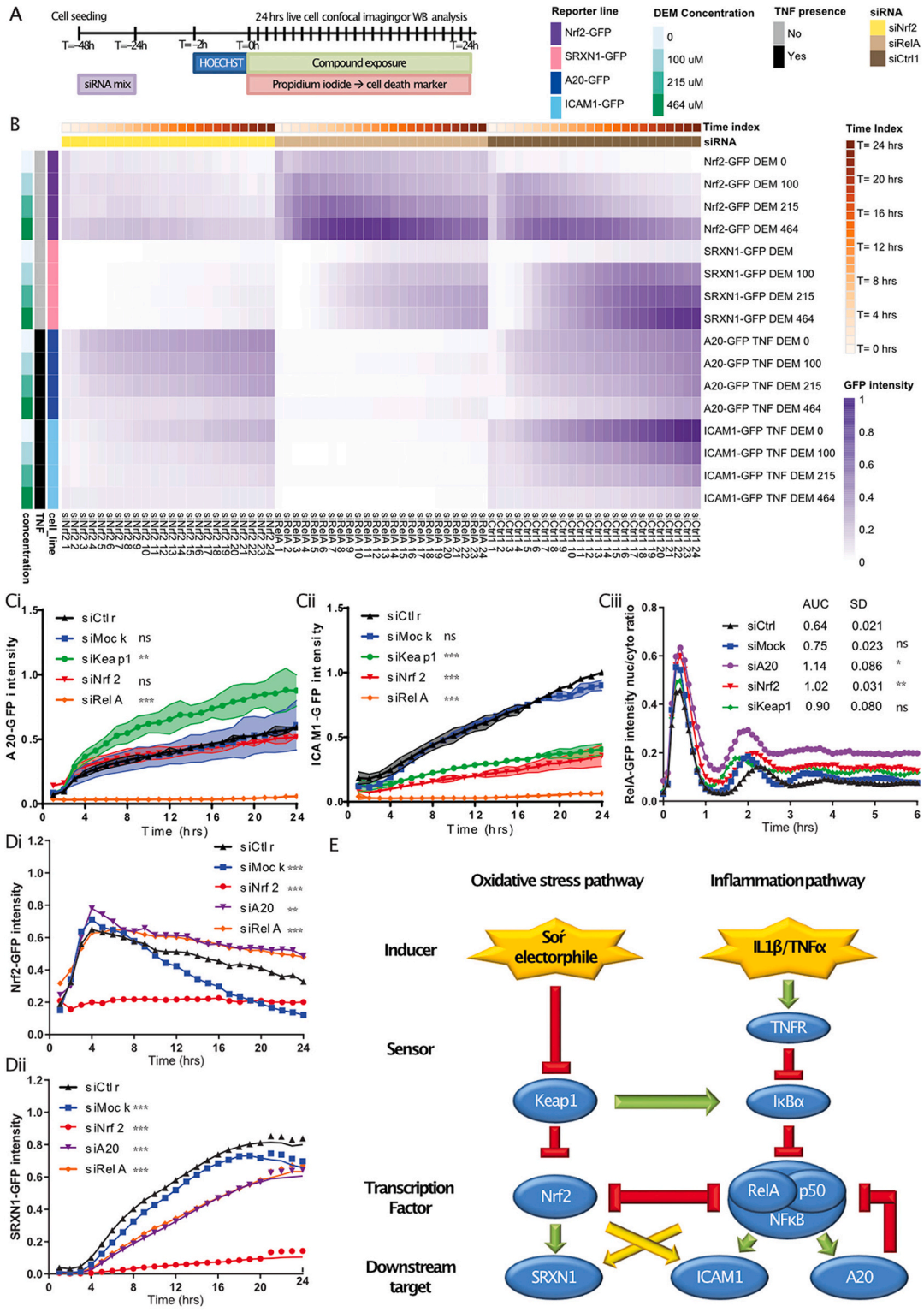

Fig. 5. Applying reporter technology in combination with siRNA mediated knockdowns to unravel the crosstalk between the oxidative stress and inflammation pathways. A) Schematic overview with the timeline and experimental procedures. A non-targeting siRNA (siCtrl1) was used as a control as well as a mock (no siRNA) reference sample. The inflammation pathway was induced with either TNFα or IL1β. Low, medium or high concentrations of DEM were used to induce the Nrf2 pathway and study the crosstalk to the inflammation pathway. In addition non-stimulated control conditions were included (DMSO). B) Hierarchical clustering (Euclidian distance) of the quantified dynamic reporter GFP data of the inflammatory and oxidative reporters after siRNA-based knockdown of key players of oxidative stress or inflammation pathway. C) Time response curves with reporter GFP intensity data (i: A20-GFP, ii: ICAM1-GFP, iii RelA-GFP), upon knockdown of interesting proteins in either the NfκB or Nrf2 pathways in the presence of TNFα. Significance was determined over the area under the time curve ($n = 3$). D) The dynamic GFP intensity plots of the Nrf2 reporters (i: Nrf2, ii: SRXN1) in the presence of DEM and TNFα (n = 3). E) The proposed schematic overview of the crosstalk between the Nrf2 and NFκB signaling pathways.

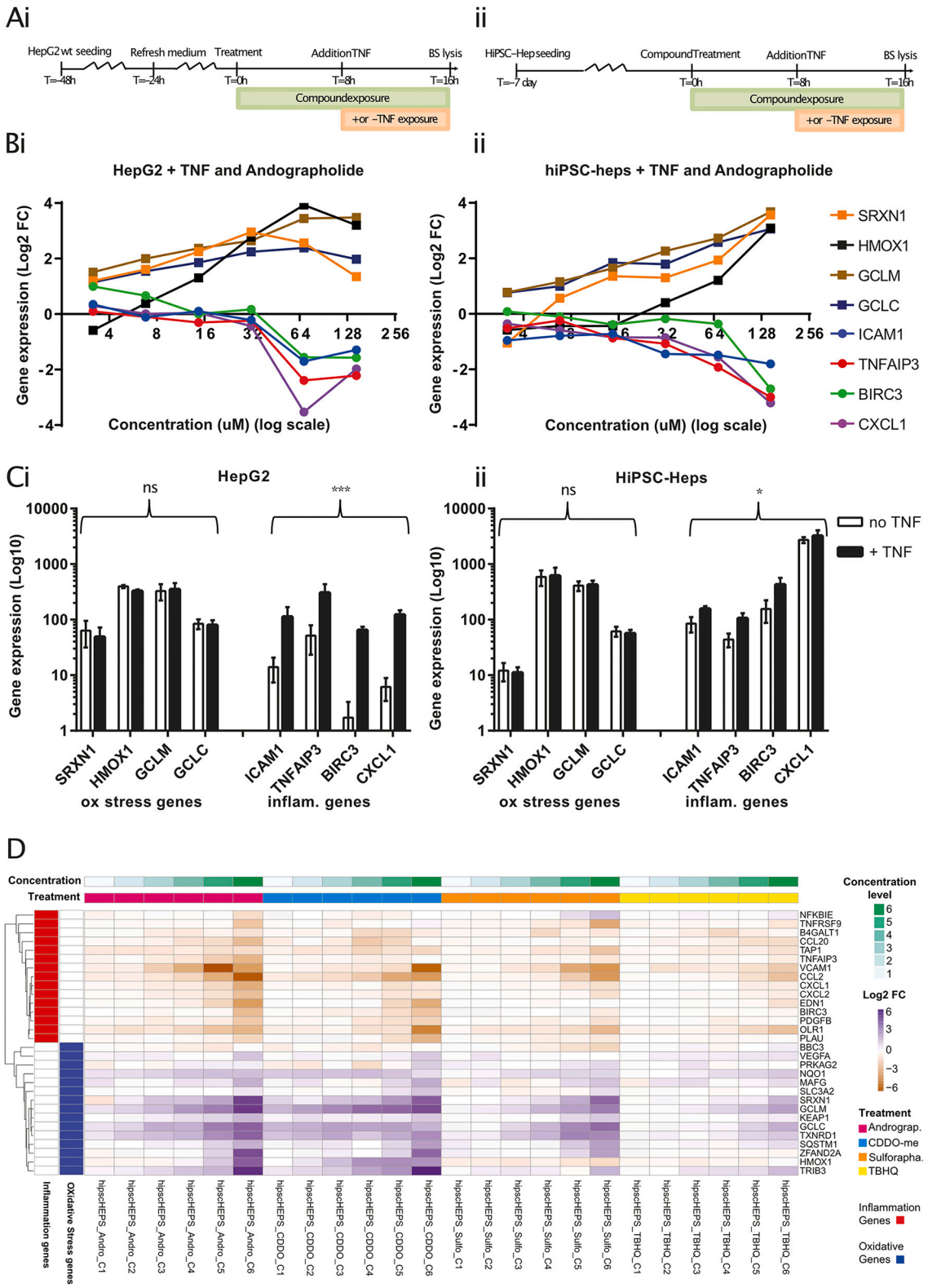

Fig. 6. Transcriptome analysis of soft electrophile treated HepG2 and hiPSC-Heps. A) Schematic overview with timelines and experimental procedures of the experiments with HepG2 wt and hiPSC-Heps (i and ii resp). B) Gene expression levels (log2FC) of downstream targets of the NFκB (circles) and Nrf2 (squares) pathways after exposure to TNFα and andrographolide in HepG2 wt and hiPSC-Heps (i and ii resp). C) Basal gene expression levels (log10) of downstream targets of the NFκB and Nrf2 pathways in the presence and absence of TNFα in HepG2 wt and hiPSC-Heps (i and ii resp). Significance is determined over the mean gene expression between the no-TNFα and TNFα conditions. D) Hierarchical clustering (Euclidian distance) of the log2 fold changes of the expression profiles of genes associated with either inflammation or oxidative stress. ($n = 3$).

activation we observed a different ranking with strong to weaker Nrf2 inducers: CDDO-me, andrographolide, sulforaphane, ethacrynic acid, DEM and TBHQ. Naturally, the in silico measurements do not reflect many important factors logP, cellular absorption and transport, chemical stability, steric hindrance, etc. that will also determine the intracellular concentration of the active molecules and, therefore, KEAP1 modification and Nrf2 activation. Our reporter assays are therefore an important asset to efficiently determine the efficacy for cellular Nrf2 activation by candidate soft electrophiles and also highlights the importance of in vitro assays to complement any in silico prediction in the first phase of chemical safety evaluation.

We found that each model compound had a very distinct oxidative stress response. CDDO-me for example caused a slow but gradual and sustained activation of Nrf2, whereas sulforaphane induced a rapid nuclear translocation of Nrf2 followed by a sharp decline. While these differences could be due to the intrinsic activities of these compounds, we cannot exclude that these differences are determined by kinetic properties of the compound such as intrinsic stability, lipophilicity, intracellular clearance. Our Nrf2-GFP reporter allows for the temporal resolution of the Nrf2 translocation thereby facilitating the characterization of pro-oxidant responses of various soft electrophiles. These different behaviors may impact on the safety aspects of soft electrophiles, in particular when repeated exposure are being considered.

Regardless of the different Nrf2 modulating properties, we observed that all our test compounds significantly inhibited the TNFα induced inflammation response, convincingly supporting the impact of Nrf2 activators on the NFκB pathway, and suggesting a crosstalk between the two pathways. A direct effect of TNFα induced NFκB signaling to the Nrf2 pathway could not be confirmed as the presence of TNFα did not influence nuclear translocation of Nrf2 nor the expression profile of the downstream target, the antioxidant SRXN1. We applied RNA interference studies to further examine a possible crosstalk. We found that depletion of KEAP1 leads to a stronger NFκB response as observed via increased levels of A20 and a higher ratio of nuclear:cytoplasmatic NFκB; treatment with DEM further enhanced this effect. This is in concordance with previous studies which proposed that depletion of KEAP1 induces accumulation and stabilization of IKKβ and thereby upregulating a NFκB response (Kim et al., 2013) (Lee et al., 2009). The suggested explanation was that Nrf2 translocation to the nucleus will bind Antioxidant Response Elements (ARE) and p300, and, thus, Nrf2 activation would lead to a depletion of p300 that would be available for p65 (Kim et al., 2013). Therefore, the competition for p300 by Nrf2 and NFκB leads to an inhibition of TNFα induced inflammation response. However, this is in contrast to a previous study by Rushworth and colleagues, in which TNFα exposures to human monocytes led to strong activation of the Nrf2 pathway (Rushworth et al., 2011). It is likely that this TNFα induced oxidative stress response is very cell type specific as it is known that inflammation is associated with systemic accumulation of reactive oxygen species (ROS) due to mitochondrial dysfunction in inflammatory cells and subsequent uncontrolled activation of NADPH oxidases (Nox1 and Nox2) (Lu et al., 2014) (Wenzel et al., 2017). Alternative explanations of NFκB pathway modulation could be the direct impact of soft electrophiles on protein sulfhydryl modifications of components of the the NFκB signaling pathway. Indeed, CDDO-me is known to directly target IKKβ in HEK293 cells at low μM concentrations, due to the modification of Cys179 of IKKβ, in association with inhibition of TNFα-induced nuclear translocation of NFκB (Yore et al., 2006). Previously we found that TNFα has a synergistic effect on diclofenac induced hepatotoxicity and inhibits the TNFα-induced nuclear translocation of the NFκB (Fredriksson et al., 2011) and through computational modelling of our data we predicted the IKK-complex to be a likely (in)direct target of this diclofenac effect (Oppelt et al., 2018). As far as we could identify, there is no information on the effect of our other soft electrophiles on IKK modulation, however, we did observe a disturbance of the IκBα oscillatory response (Fig. 3D) possibly due to perturbations of the IKK-complex-mediated phosphorylation of IκBα, which would support this concept.

In conclusion, our data indicate that different soft electrophiles induced the Nrf2 pathway and at higher concentrations suppress the inflammation associated NFκB pathway. This latter activity may have adverse consequences for proper systemic immune regulation with respect for drug development and natural product discovery that target KEAP1 to selectively modulate the Nrf2 pathway. Our current HepG2 reporter panel in combination with dynamic imaging can support the identification of Nrf2 pathway activation selectivity and defining most optimal safety margins in a cost effective high throughput manner.

Declaration of Competing Interest

The described HepG2 BAC GFP reporters are now licensed to Toxys. B.t.B is currently employed at this company.

Acknowledgements

This work was financially supported by the European Commission Horizon2020 projects EU-ToxRisk project (grant agreement no. 681002) and RISK-HUNT3R (grant agreement no. 964537).

Appendix A. Supplementary data

Supplementary data to this article can be found online at https://doi.org/10.1016/j.tiv.2022.105419.

References

Afonina, I.S., Zhong, Z., Karin, M., Beyaert, R., 2017. Limiting inflammation - the negative regulation of NF-B and the NLRP3 inflammasome. Nat. Immunol. 18, 861–869. https://doi.org/10.1038/ni.3772.

Burgess, A., Shah, K., Hough, O., Hynynen, K., 2016. Aurora B regulates Formin mDia3 in achieving metaphase chromosome alignment Lina. Free Radic. Biol. Med. 15, 477–491. https://doi.org/10.1586/14737175.2015.1028369.Focused.

Di, Z., Herpers, B., Fredriksson, L., Yan, K., van de Water, B., Verbeek, F.J., Meerman, J. H.N., 2012. Automated analysis of NF-κB nuclear translocation kinetics in high-throughput screening. PLoS One 7. https://doi.org/10.1371/journal.pone.0052337.

Fredriksson, L., Herpers, B., Benedetti, G., Matadin, Q., Puigvert, J.C., de Bont, H., Dragovic, S., Vermeulen, N.P.E., Commandeur, J.N.M., Danen, E., De Graauw, M., Van de Water, B., 2011. Diclofenac inhibits tumor necrosis factor-α-induced nuclear factor-κB activation causing synergistic hepatocyte apoptosis. Hepatology 53, 2027–2041. https://doi.org/10.1002/hep.24314.

Fredriksson, L., Wink, S., Herpers, B., Benedetti, G., Hadi, M., De Bont, H., Groothuis, G., Luijten, M., Danen, E., De Graauw, M., Meerman, J., van de Water, B., 2014. Drug-induced endoplasmic reticulum and oxidative stress responses independently sensitize toward TNFα-mediated hepatotoxicity. Toxicol. Sci. 140, 144–159. https://doi.org/10.1093/toxsci/kfu072.

Guerrero-Beltrán, C.E., Calderón-Oliver, M., Pedraza-Chaverri, J., Chirino, Y.I., 2012. Protective effect of sulforaphane against oxidative stress: recent advances. Exp. Toxicol. Pathol. https://doi.org/10.1016/j.etp.2010.11.005.

Han, Y., Englert, J.A., Delude, R.L., Fink, M.P., 2005. Ethacrynic acid inhibits multiple steps in the NF-κB signaling pathway. Shock 23, 45–53. https://doi.org/10.1097/01.shk.0000150629.53699.3f.

Herpers, B., Wink, S., Fredriksson, L., Di, Z., Hendriks, G., Vrieling, H., de Bont, H., van de Water, B., 2016. Activation of the Nrf2 response by intrinsic hepatotoxic drugs correlates with suppression of NF-κB activation and sensitizes toward TNFα-induced cytotoxicity. Arch. Toxicol. 90, 1163–1179. https://doi.org/10.1007/s00204-015-1536-3.

Hiemstra, S., Niemeijer, M., Koedoot, E., Wink, S., Klip, J.E., Vlasveld, M., De Zeeuw, E., Van Os, B., White, A., van de Water, B., 2017. Comprehensive landscape of Nrf2 and p53 pathway activation dynamics by oxidative stress and DNA damage. Chem. Res. Toxicol. 30, 923–933. https://doi.org/10.1021/acs.chemrestox.6b00322.

Higa, A., Chevet, E., 2012. Redox signaling loops in the unfolded protein response. Cell. Signal. https://doi.org/10.1016/j.cellsig.2012.03.011.

Jones, J.J., Fan, J., Nathens, A.B., Kapus, A., Shekhman, M., Marshall, J.C., Parodo, J., Rotstein, O.D., 1999. Redox manipulation using the thiol-oxidizing agent diethyl maleate prevents hepatocellular necrosis and apoptosis in a rodent endotoxemia model. Hepatology 30, 714–724. https://doi.org/10.1002/hep.510300324.

Kim, S.W., Lee, H.K., Shin, J.H., Lee, J.K., 2013. Up-down regulation of HO-1 and iNOS gene expressions by ethyl pyruvate via recruiting p300 to Nrf2 and depriving it from p65. Free Radic. Biol. Med. 65, 468–476. https://doi.org/10.1016/j.freeradbiomed.2013.07.028.

Kobayashi, E.H., Suzuki, T., Funayama, R., Nagashima, T., Hayashi, M., Sekine, H., Tanaka, N., Moriguchi, T., Motohashi, H., Nakayama, K., Yamamoto, M., 2016. Nrf2 suppresses macrophage inflammatory response by blocking proinflammatory

cytokine transcription. Nat. Commun. 7, 1–14. https://doi.org/10.1038/ncomms11624.
Kolde, R., 2012. Pheatmap: pretty heatmaps. R Packag. version 61.
Lee, D., Kuo, H., Liu, M., Chou, C., Xia, W., Shen, J., Chen, C., Huo, L., Hsu, M., Li, C., Ding, Q., Liao, T., Lai, C., Lin, A., Chang, Y., 2009. NIH Public Access. Mol. Cell 36, 131–140. https://doi.org/10.1016/j.molcel.2009.07.025.KEAP1.
Lerebours, F., Vacher, S., Andrieu, C., Espie, M., Marty, M., Lidereau, R., Bieche, I., 2008. NF-kappa B genes have a major role in inflammatory breast cancer. BMC Cancer 8, 1–11. https://doi.org/10.1186/1471-2407-8-41.
Li, B., Jiang, T., Liu, H., Miao, Z., Fang, D., Zheng, L., Zhao, J., 2018. Andrographolide protects chondrocytes from oxidative stress injury by activation of the Keap1–Nrf2–are signaling pathway. J. Cell. Physiol. 234, 561–571. https://doi.org/10.1002/jcp.26769.
Lopachin, R.M., Gavin, T., 2017. Thiolate sites : relevance to pathophysiological. Free Radic. Res. 50, 195–205. https://doi.org/10.3109/10715762.2015.1094184.REACTIONS.
Lu, C.Y., Yang, Y.C., Li, C.C., Liu, K.L., Lii, C.K., Chen, H.W., 2014. Andrographolide inhibits TNFα-induced ICAM-1 expression via suppression of NADPH oxidase activation and induction of HO-1 and GCLM expression through the PI3K/Akt/Nrf2 and PI3K/Akt/AP-1 pathways in human endothelial cells. Biochem. Pharmacol. 91, 40–50. https://doi.org/10.1016/j.bcp.2014.06.024.
Maeda, Y., Takeyoshi, M., Chuma, T., Iwata, H., 2020. α-Sens: the improved ARE-Nrf2-based sensitization screening assay using normalized transcriptional activity. Toxicology 439, 152476. https://doi.org/10.1016/j.tox.2020.152476.
Niemeijer, M., Hiemstra, S., Wink, S., Den Hollander, W., ter Braak, B., van de Water, B., 2018. Springer Protocols Systems Microscopy Approaches in Unraveling and Predicting DILI. Springer Protoc.
Oppelt, Angela, Kaschek, Daniel, Huppelschoten, Suzanna, Sison-Young, Rowena, Zhang, Fang, Buck-Wiese, Marie, Herrmann, Franziska, Malkusch, Sebastian, Krüger, Carmen L., Meub, Mara, Merkt, Benjamin, Zimmermann, Lea, Schofield, Amy, Jones, Robert P., Malik, Hassan, Schilling, Marcel, Heilemann, Mike, Water, Bob van de, Goldring, Christopher E., Park, B. Kevin, Timmer, Jens, Klingmüller, Ursula, 2018. Model-based identification of TNFα-induced IKKβ-mediated and IκBα-mediated regulation of NFκB signal transduction as a tool to quantify the impact of drug-induced liver injury compounds. NPJ Syst. Biol. Appl. 4 (1), 152. https://doi.org/10.1038/s41540-018-0058-z.
Patlewicz, G., Kuseva, C., Kesova, A., Popova, I., Zhechev, T., Pavlov, T., Roberts, D.W., Mekenyan, O., 2014. Towards AOP application - implementation of an integrated approach to testing and assessment (IATA) into a pipeline tool for skin sensitization. Regul. Toxicol. Pharmacol. 69, 529–545. https://doi.org/10.1016/j.yrtph.2014.06.001.
Poser, I., Pozniakovsky, A., Weigl, D., Nitzsche, A., Hegemann, B., Augsburg, M., Sykora, M.M., Hofemeister, H., Zhang, Y., Peters, J., Buchholz, F., Hyman, A.A., 2008. BAC TransgeneOmics : a high-throughput method for exploration of protein function in mammals. Nat. Methods 5, 409–415. https://doi.org/10.1038/nmeth.1199.BAC.
Rushworth, S.A., Shah, S., MacEwan, D.J., 2011. Correction: TNF mediates the sustained activation of Nrf2 in human monocytes. J. Immunol. 187, 6160. https://doi.org/10.4049/jimmunol.1190072.
Rushworth, S.A., Zaitseva, L., Murray, M.Y., Shah, N.M., Bowles, K.M., Macewan, D.J., Dc, W., 2014. The high Nrf2 expression in human acute myeloid leukemia is driven by NF- κ B and underlies its chemo-resistance The high Nrf2 expression in human acute myeloid leukemia is driven by NF- κ B and underlies its chemo-resistance, 120, pp. 5188–5198. https://doi.org/10.1182/blood-2012-04-422121.
Srivastava, N., Akhila, A., 2010. Biosynthesis of andrographolide in Andrographis paniculata. Phytochemistry 71, 1298–1304. https://doi.org/10.1016/j.phytochem.2010.05.022.
ter Braak, B., Niemeijer, M., Boon, R., Parmentier, C., Baze, A., Richert, L., Huppelschoten, S., Wink, S., Verfaillie, C., van de Water, B., 2021a. Systematic transcriptome-based comparison of cellular adaptive stress response activation networks in hepatic stem cell-derived progeny and primary human hepatocytes. Toxicol. in Vitro 73. https://doi.org/10.1016/j.tiv.2021.105107.
ter Braak, B., Niemeijer, M., Wolters, L., Le Dévédec, S., Bouwman, P., van de Water, B., 2021b. Towards an advanced testing strategy for genotoxicity using image-based 2D and 3D HepG2 DNA damage response fluorescent protein reporters. Mutagenesis. https://doi.org/10.1093/mutage/geab031.
Thimmulappa, R.K., Lee, H., Rangasamy, T., Reddy, S.P., Yamamoto, M., Kensler, T.W., Biswal, S., 2006. Nrf2 is a critical regulator of the innate immune reponse and survival during experimental sepsis. J. Clin. Invest. 2006, 116. https://doi.org/10.1172/JCI25790.984.
Turley, A.E., Zagorski, J.W., Rockwell, C.E., 2016. The Nrf2 activator tBHQ inhibits T cell activation of primary human CD4 T cells. Cytokin 71, 289–295. https://doi.org/10.1016/j.cyto.2014.11.006.The.
Wenzel, P., Kossmann, S., Münzel, T., Daiber, A., 2017. Redox regulation of cardiovascular inflammation – immunomodulatory function of mitochondrial and Nox-derived reactive oxygen and nitrogen species. Free Radic. Biol. Med. 109, 48–60. https://doi.org/10.1016/j.freeradbiomed.2017.01.027.
Wickham, H., 2009. ggplot2: Elegant Graphics for Data Analysis. Springer-Verlag, New York.
Wink, S., Hiemstra, S., Huppelschoten, S., Danen, E., Hendriks, G., Vrieling, H., Herpers, B., Van De Water, B., 2014. Quantitative high content imaging of cellular adaptive stress response pathways in toxicity for chemical safety assessment quantitative high content imaging of cellular adaptive stress response pathways in Division of Toxicology, Leiden Academic Centre f. Chem. Res. Toxicol. 27, 338–355. https://doi.org/10.1021/tx4004038.
Wink, S., Hiemstra, S., Herpers, B., van de Water, B., 2017. High-content imaging-based BAC-GFP toxicity pathway reporters to assess chemical adversity liabilities. Arch. Toxicol. 91, 1367–1383. https://doi.org/10.1007/s00204-016-1781-0.
Wu, R.P., Hayashi, T., Cottam, H.B., Jin, G., Yao, S., Wu, C.C.N., Rosenbach, M.D., Corr, M., Schwab, R.B., Carson, D.A., 2010. Nrf2 responses and the therapeutic selectivity of electrophilic compounds in chronic lymphocytic leukemia. Proc. Natl. Acad. Sci. 107, 7479–7484. https://doi.org/10.1073/pnas.1002890107.
Yamamoto, M., Kensler, T.W., Motohashi, H., 2018. The KEAP1-NRF2 system: a thiol-based sensor-effector apparatus for maintaining redox homeostasis. Physiol. Rev. 98, 1169–1203. https://doi.org/10.1152/physrev.00023.2017.
Yeakley, J.M., Shepard, P.J., Goyena, D.E., Vansteenhouse, H.C., McComb, J.D., Seligmann, B.E., 2017. A Trichostatin a expression signature identified by TempO-Seq targeted whole transcriptome profiling. PLoS One 12. https://doi.org/10.1371/journal.pone.0178302.
Yore, M.M., Liby, K.T., Honda, T., Gribble, G.W., Sporn, M.B., 2006. The synthetic triterpenoid 1-[2-cyano-3,12-dioxooleana-1,9(11)-dien-28-oyl]imidazole blocks nuclear factor-κB activation through direct inhibition of IκB kinase β. Mol. Cancer Ther. 5, 3232–3239. https://doi.org/10.1158/1535-7163.MCT-06-0444.
Zeeuw De, D., Vaziri, N.D., Wrolstad, D., Wanner, C., Houser, M., Goldsberry, A., Chertow, G.M., Krauth, M., Lambers Heerspink, H.J., Wittes, J., de Zeeuw, D., McMurray, J.J., Christ-Schmidt, H., Bakris, G.L., Chin, M., Meyer, C.J., Audhya, P., Toto, R.D., Remuzzi, G., Akizawa, T., Parving, H.-H., 2013. Bardoxolone methyl in type 2 diabetes and stage 4 chronic kidney disease. N. Engl. J. Med. 369, 2492–2503. https://doi.org/10.1056/nejmoa1306033.